

# Quantum correlations and speed limit of central spin system

Devvrat Tiwari,<sup>1,\*</sup> K.G Paulson,<sup>1,†</sup> and Subhashish Banerjee<sup>1,‡</sup>

<sup>1</sup>Indian Institute of Technology Jodhpur-342030, India

(Dated: May 27, 2022)

In this article we consider single and two qubit central spin systems interacting with fermionic baths and discuss their dynamical properties. We consider the cases of interacting and non-interacting fermionic spin baths, and investigate the quantum speed limit (QSL) time of evolution. The impact of size of the spin bath on quantum speed limit for single qubit central spin model is analyzed. We estimate the quantum correlations for (non-)interacting two central spin qubits, and compare their dynamical behavior with that of QSL time under various conditions. We show how QSL time could be availed to analyze the dynamics of quantum correlations.

## I. INTRODUCTION

Evolution of a quantum system almost inevitably involves the influence of its ambient environment. This is handled in a consistent manner by the theory of open quantum systems [1, 2]. Open system ideas find use in a wide range of fields ranging from quantum optics [3, 4], to condensed matter [5, 6], quantum statistical physics [7–9], particle physics [10–15], cosmology [16, 17], quantum chemistry [18–20] and quantum biology [21]. In the last decade, its applications to the field of quantum information have seen a phenomenal growth [22–30]. The quantum system’s coupling to the reservoir (bath or environment) plays a significant role in deciding the nature of its dynamics, Markovian or non-Markovian [31–35], and the usefulness of quantum resources for technological advancements.

The dynamics of quantum correlations under the (non-)Markovian environment have been extensively studied [36–38]. The non-Markovian behavior, arising from, say, a strong system-bath coupling, can delay the decay and sometimes source the revival of quantum correlations [39]. The evolution of the system of interest can change due to the nature of the bath, and this could be witnessed from the dynamics of quantum speed limit (QSL) time [40]. QSL time, the minimum time required for the evolution between two states finds many potential applications [41–43] in the field of quantum information and computation and is an active research topic.

In general, comprehending the subtlety of the environment’s impact on the quantum system is a non-trivial task. In this work, we discuss the central spin system, both single as well as double spin systems, interacting with fermionic bath(s) and investigate the corresponding evolution under various conditions. The class of fermionic bath models [44] are of immense interest in the quantum theory of magnetism [45], quantum spin glasses [46], theory of conductors and superconductors [47]. This work investigates the QSL time and the dynamics of quantum correlations of the central spin system interacting with the fermionic bath. It is motivated by a model of quantum thermal diode [48]. We consider the single as well as interacting two central spin systems interacting with their

corresponding bath(s), with both non-interacting and interacting bath spins. This is used to contrast and characterize the quantum statistical mechanics of the central spin model. The presence of bath spin interactions is seen to contribute significantly to the dynamics. This sets apart the fermionic bath from its bosonic counterpart. For the two central spin system we will see that, it is fruitful to consider the dynamics as local or global depending on the absence or presence of the spin-spin interaction. Quantum correlations, in particular, entanglement and discord, are calculated and their connection with QSL time under different conditions is discussed.

The present work is structured as follows: In Sec. II, we discuss the details of the single and two qubit central spin model under the influence of local and global baths and their operator-sum representations. Section III studies the characterization of the central spin model and the impact of bath spin interactions. Investigation of QSL time for the single and two qubit central spin system is given in Sec. IV, followed by the discussion of dynamics of quantum correlations in Sec. V. In Sec. VI, the connection between quantum correlations and QSL time is discussed, followed by the conclusion.

## II. THE MODEL

In this section, we present the central spin model, that is, a spin-1/2 particle (central spin) coupled to a thermal bath of spin-1/2 particles. The central spin interacts uniformly with the bath spins. We discuss the dynamics of single and two qubit central spin models. The bath spins in these models can be interacting as well as non-interacting.

### A. Single qubit central spin model

We consider a single central spin interacting uniformly and centrally with a spin bath and the bath spins also interact with

\* devvrat.1@iitj.ac.in

† paulsonkgeorg@gmail.com

‡ subhashish@iitj.ac.in

each other. The Hamiltonian of this system is given by

$$\begin{aligned}
H_{\text{single}} &= H_S + H_E + H_{SE}, \\
&= \frac{\hbar}{2}\omega_0\sigma_0^z + \frac{\hbar\omega}{2N}\sum_{i=1}^N\left\{\frac{1}{2}\sum_{\substack{j=1 \\ j\neq i}}^N(\sigma_i^x\sigma_j^x + \sigma_i^y\sigma_j^y) + \sigma_i^z\right\} \\
&\quad + \frac{\hbar\epsilon}{2\sqrt{N}}\sum_{i=1}^N(\sigma_0^x\sigma_i^x + \sigma_0^y\sigma_i^y),
\end{aligned} \tag{1}$$

where  $H_S$ ,  $H_E$  and  $H_{SE}$  are the system, environment and interaction Hamiltonians, respectively. Here  $\sigma_0^k$  ( $k = x, y, z$ ) represents the Pauli spin matrices for the central spin system and  $\sigma_i^k$  are the Pauli spin matrices for the  $i^{\text{th}}$  spin of the bath.  $N$  represents the number of spins in the bath. The frequency of the bath and the bath-spin interaction strength are rescaled as  $\omega/N$  and  $\epsilon/\sqrt{N}$ , respectively. The above single qubit central spin model is an extension of the model given in [49] with the added condition that the bath spins also interact with each other. Using collective momentum operator for the bath spins, we can rewrite the interaction and bath Hamiltonians as

$$\begin{aligned}
H_{SE} &= \frac{\hbar\epsilon}{2\sqrt{N}}(\sigma_0^x J_x + \sigma_0^y J_y), \\
H_E &= \hbar\omega\left(\frac{J_+ J_-}{N} - \frac{\mathbb{I}}{2}\right).
\end{aligned} \tag{2}$$

We then redefine the collective angular momentum operators using Holstein-Primakoff transformations as

$$J_+ = \sqrt{N}a^\dagger\sqrt{1 - \frac{a^\dagger a}{2N}}, \quad J_- = \sqrt{N}\sqrt{1 - \frac{a^\dagger a}{2N}}a, \tag{3}$$

where  $a$  and  $a^\dagger$  are the bosonic annihilation and creation operators. We can now rewrite the Hamiltonians in Eq. (2), in terms of  $a$  and  $a^\dagger$ , as

$$\begin{aligned}
H_{SE} &= \hbar\epsilon\left[\sigma_0^+\sqrt{1 - \frac{a^\dagger a}{2N}}a + \sigma_0^-\sqrt{1 - \frac{a^\dagger a}{2N}}\right], \\
H_E &= \hbar\omega\left[a^\dagger a\left(1 - \frac{a^\dagger a - 1}{2N}\right) - \frac{\mathbb{I}}{2}\right].
\end{aligned} \tag{4}$$

Following [49–51], we derive the exact reduced dynamics of the central spin system. The reduced state of the central spin system after the evolution of the total system and bath state is given as

$$\begin{aligned}
\rho_S(t) &= \text{Tr}_B(e^{-iHt/\hbar}\rho_S(0) \otimes \rho_E(0)e^{iHt/\hbar}), \\
&= \begin{pmatrix} \rho_{11}(t) & \rho_{12}(t) \\ \rho_{21}(t) & \rho_{22}(t) \end{pmatrix},
\end{aligned} \tag{5}$$

where

$$\begin{aligned}
\rho_{11}(t) &= a_1(t)\rho_{11}(0) + d_1(t)\rho_{22}(0), \\
\rho_{12}(t) &= \gamma_1(t)\rho_{12}(0).
\end{aligned} \tag{6}$$

Here

$$\begin{aligned}
a_1(t) &= \frac{1}{Z}\sum_{n=0}^N |A_1(n, t)|^2 e^{-\frac{\hbar\omega}{kT}(n(1-\frac{n-1}{2N})-\frac{1}{2})}, \\
d_1(t) &= \frac{1}{Z}\sum_{n=0}^N n|D_1(n, t)|^2 e^{-\frac{\hbar\omega}{kT}(n(1-\frac{n-1}{2N})-\frac{1}{2})}, \\
\gamma_1(t) &= \frac{1}{Z}\sum_{n=0}^N A_1(n, t)C_1^*(n, t)e^{-\frac{\hbar\omega}{kT}(n(1-\frac{n-1}{2N})-\frac{1}{2})},
\end{aligned} \tag{7}$$

with

$$\begin{aligned}
A_1(n, t) &= e^{-in\omega(1-\frac{n}{2N})t}\left[-i\left\{\omega_0 - \omega\left(1 - \frac{n}{N}\right)\right\}\right. \\
&\quad \times \left.\frac{\sin(\eta t/2)}{\eta} + \cos(\eta t/2)\right], \\
C_1(n, t) &= e^{-i(n-1)\omega(1-\frac{n}{2N})t}\left[i\left\{\omega_0 - \omega\left(1 - \frac{n-1}{N}\right)\right\}\right. \\
&\quad \times \left.\frac{\sin(\eta' t/2)}{\eta'} + \cos(\eta' t/2)\right], \\
D_1(n, t) &= -2i\epsilon\sqrt{1 - \frac{n-1}{2N}}e^{-i(n-1)\omega(1-\frac{n}{2N})t}\frac{\sin(\eta' t/2)}{\eta'},
\end{aligned} \tag{8}$$

where

$$\begin{aligned}
\eta &= \sqrt{\left\{\omega_0 - \omega\left(1 - \frac{n}{N}\right)\right\}^2 + 4\epsilon^2(n+1)\left(1 - \frac{n}{2N}\right)}, \\
\eta' &= \sqrt{\left\{\omega_0 - \omega\left(1 - \frac{n-1}{N}\right)\right\}^2 + 4\epsilon^2n\left(1 - \frac{n-1}{2N}\right)}.
\end{aligned} \tag{9}$$

We now construct the dynamical map of the evolution for the central spin system. To this end, we represent the evolution of the reduced system by the Kraus operator sum representation, given as  $\rho(t) = \sum_i K_i(t)\rho(0)K_i^\dagger(t)$ . In the particular case given above, we can write the Kraus operators as

$$\begin{aligned}
K_1(t) &= \sqrt{d_1(t)}\begin{pmatrix} 0 & 1 \\ 0 & 0 \end{pmatrix}, \\
K_2(t) &= \sqrt{b_1(t)}\begin{pmatrix} 0 & 0 \\ 1 & 0 \end{pmatrix},
\end{aligned}$$

$$K_3(t) = \sqrt{\frac{R_1}{1+T_1^2}}\begin{pmatrix} T_1 e^{i\theta} & 0 \\ 0 & 1 \end{pmatrix},$$

$$K_4(t) = \sqrt{\frac{R_2}{1+T_2^2}}\begin{pmatrix} T_2 e^{i\theta} & 0 \\ 0 & 1 \end{pmatrix}, \tag{10}$$

where

$$b_1(t) = \frac{1}{Z}\sum_{n=0}^N (n+1)|B_1(n, t)|^2 e^{-\frac{\hbar\omega}{kT}(n(1-\frac{n-1}{2N})-\frac{1}{2})}, \tag{11}$$

such that

$$B_1(n, t) = -2i\epsilon \sqrt{1 - \frac{n}{2N}} e^{-in\omega(1 - \frac{n}{2N})t} \frac{\sin(\eta t/2)}{\eta}, \quad (12)$$

and  $\theta = \arctan(\gamma_1 I(t)/\gamma_1 R(t))$ . Further,

$$\begin{aligned} R_{1,2}(t) &= \frac{a_1(t) + c_1(t) \pm \sqrt{(a_1(t) - c_1(t))^2 + 4|\gamma_1(t)|^2}}{2}, \\ T_{1,2}(t) &= \frac{a_1(t) - c_1(t) \pm \sqrt{(a_1(t) - c_1(t))^2 + 4|\gamma_1(t)|^2}}{2|\gamma_1(t)|}, \end{aligned} \quad (13)$$

where

$$c_1(t) = \frac{1}{Z} \sum_{z=0}^N |C_1(n, t)|^2 e^{-\frac{\hbar\omega}{kT}(n(1 - \frac{n}{2N}) - \frac{1}{2})}. \quad (14)$$

We can also consider a single qubit central spin system interacting with a non-interacting bath. The Hamiltonian for this system is given by

$$\begin{aligned} H'_{\text{single}} &= H_S + H'_E + H_{SE}, \\ &= \frac{\hbar}{2} \omega_0 \sigma_0^z + \frac{\hbar\omega}{2N} \sum_{i=1}^N \sigma_i^z + \frac{\hbar\epsilon}{2\sqrt{N}} \sum_{i=1}^N (\sigma_0^x \sigma_i^x + \sigma_0^y \sigma_i^y), \end{aligned} \quad (15)$$

Exact dynamics of this particular system is derived in [49]. We represent the reduced state of the system in this case by density matrix  $\rho'_S(t)$  and the Kraus operator sum representation by

$$\rho'_S(t) = \sum_i K'_i(t) \rho(0) K_i'^{\dagger}(t). \quad (16)$$

The form of these Kraus operators are the same as given in [49].

## B. Two qubit central spin model

We now consider two central spin-1/2 particles interacting uniformly with two separate spin baths. We divide the model into two categories, *viz.* local and global bath scenarios depending upon the (non-)interaction between the two central spins [52]. Further, we also differentiate the above models based upon the interaction of bath spins with each other.

### 1. Local bath scenario

Here we consider two central spins ( $A$  and  $B$ ) with frequencies  $\omega_{0A}$  and  $\omega_{0B}$  interacting uniformly with their respective local baths ( $N_A$  and  $N_B$ ) with frequencies  $\omega_A$  and  $\omega_B$ .  $\epsilon_A$  and  $\epsilon_B$  are the interaction strengths for the interaction between each central spin and its local bath. We first consider the case where the spins of each bath interact among themselves and no interaction between both the central spins. We derive the dynamical map in this case by solving the local Lindblad equations

for each central spin. The dynamics of the reduced state of such a system is given by

$$\rho_{AB}(t) = \sum_{k=1}^{16} E_k(t) \rho_{AB}(0) E_k^{\dagger}(t), \quad (17)$$

where  $\sum_{k=1}^{16} E_k = \sum_{i=1}^4 \sum_{j=1}^4 K_i^A \otimes K_j^B$ .  $K_i^A$ 's and  $K_j^B$ 's are the Kraus operators given in Eq. (10).

We next consider the case where the spins of the individual baths are non-interacting with no interaction between the central spins. To this end, the dynamics of the reduced state is given as

$$\rho'_{AB}(t) = \sum_{k=1}^{16} E'_k(t) \rho'_{AB}(0) E_k'^{\dagger}(t), \quad (18)$$

where  $\sum_{k=1}^{16} E'_k = \sum_{i=1}^4 \sum_{j=1}^4 K_i^A \otimes K_j^B$ .  $K_i^A$ 's and  $K_j^B$ 's are the Kraus operators given in Eq. (16).

### 2. Global bath scenario

Here each central spin is uniformly coupled to its respective bath and also interact with each other. First, we consider the case where spins of the individual baths interact with each other. The Hamiltonian for this particular case is given by

$$\begin{aligned} \mathcal{H} &= H_{S_1} + H_{S_2} + H_{S_1 S_2} + H_{E_1} + H_{E_2} + H_{S_1 E_1} + H_{S_2 E_2}, \\ &= \frac{\hbar\omega_1}{2} \sigma_{01}^z + \frac{\hbar\omega_2}{2} \sigma_{02}^z + \frac{\hbar\delta}{2} (\sigma_{01}^z \otimes \sigma_{02}^z) \\ &\quad + \frac{\hbar\omega_a}{2M} \sum_{i=1}^M \left[ \frac{1}{2} \sum_{\substack{j=1 \\ j \neq i}}^M (\sigma_{i1}^x \sigma_{j1}^x + \sigma_{i1}^y \sigma_{j1}^y) + \sigma_{i1}^z \right] \\ &\quad + \frac{\hbar\omega_b}{2N} \sum_{i=1}^N \left[ \frac{1}{2} \sum_{\substack{j=1 \\ j \neq i}}^N (\sigma_{i2}^x \sigma_{j2}^x + \sigma_{i2}^y \sigma_{j2}^y) + \sigma_{i2}^z \right] \\ &\quad + \frac{\hbar\epsilon_1}{2\sqrt{M}} \sum_{i=1}^M (\sigma_{01}^x \sigma_{i1}^x + \sigma_{01}^y \sigma_{i1}^y) \\ &\quad + \frac{\hbar\epsilon_2}{2\sqrt{N}} \sum_{i=1}^N (\sigma_{02}^x \sigma_{i2}^x + \sigma_{02}^y \sigma_{i2}^y), \end{aligned} \quad (19)$$

where  $\sigma_{il}^k$  ( $k = x, y, z$ ;  $l = 1, 2$ ) are Pauli matrices corresponding to  $i^{\text{th}}$  spin of the  $l^{\text{th}}$  bath, and  $\sigma_{0l}^k$  are Pauli matrices for  $l^{\text{th}}$  central spin.  $\omega_{a,b}$  are bath frequencies of two spin baths and  $\epsilon_{1,2}$  are interaction parameters of the respective spin-bath interaction.  $M$  and  $N$  are the respective number of spins in two baths. The dynamical map of the above system was derived in [51]. The reduced state of the system composed of two central spins after global unitary evolution of the joint central spin-bath state, in terms of Kraus operator sum representation, is given by

$$\rho_{S_1 S_2}(t) = \sum_{i=1}^{16} G_i \rho_{S_1 S_2}(0) G_i^{\dagger}, \quad (20)$$

where the  $G_i$ 's are the Kraus operators for the evolution of the reduced state of the system. These Kraus operators can be obtained numerically, as in [51].

Finally, we consider a similar model but with non interacting bath spins. The Hamiltonian in this case is given by

$$\begin{aligned} \mathcal{H}' &= H_{S_1} + H_{S_2} + H_{S_1 S_2} + H'_{E_1} + H'_{E_2} + H_{S_1 E_1} + H_{S_2 E_2}, \\ &= \frac{\hbar\omega_1}{2}\sigma_{01}^z + \frac{\hbar\omega_2}{2}\sigma_{02}^z + \frac{\hbar\delta}{2}(\sigma_{01}^z \otimes \sigma_{02}^z) + \frac{\hbar\omega_a}{2M} \sum_{i=1}^M \sigma_{i1}^z \\ &+ \frac{\hbar\omega_b}{2N} \sum_{i=1}^N \sigma_{i2}^z + \frac{\hbar\epsilon_1}{2\sqrt{M}} \sum_{i=1}^M (\sigma_{01}^x \sigma_{i1}^x + \sigma_{01}^y \sigma_{i1}^y) \\ &+ \frac{\hbar\epsilon_2}{2\sqrt{N}} \sum_{i=1}^N (\sigma_{02}^x \sigma_{i2}^x + \sigma_{02}^y \sigma_{i2}^y). \end{aligned} \quad (21)$$

The above Hamiltonian can also be solved using the technique used to solve the model in Eq. (19). Here the bath Hamiltonians,  $H'_{E_1}$  and  $H'_{E_2}$  are given in terms of collective angular momentum operators as

$$H'_{E_1} = \frac{\hbar\omega_a}{2M} J_{z1}, \quad H'_{E_2} = \frac{\hbar\omega_b}{2N} J_{z2}, \quad (22)$$

and these can be rewritten using Holstein-Primakoff transformation as

$$\begin{aligned} H'_{E_1} &= -\frac{\hbar\omega_a}{2} \left(1 - \frac{a^\dagger a}{M}\right), \\ H'_{E_2} &= -\frac{\hbar\omega_b}{2} \left(1 - \frac{b^\dagger b}{N}\right). \end{aligned} \quad (23)$$

The corresponding Kraus operator sum representation is given as

$$\rho'_{S_1 S_2}(t) = \sum_{i=1}^{16} G'_i \rho'_{S_1 S_2}(0) G_i'^{\dagger}. \quad (24)$$

These Kraus operators  $G'_i$ 's can be obtained numerically using a similar approach.

### III. CHARACTERIZATION OF CENTRAL SPIN MODEL: IMPACT OF BATH SPIN INTERACTIONS

Here, we study the quantum statistical nature of the central spin models. We use trace distance and von Neumann entropy to identify the changes in the single qubit and the two qubit central spin models, caused by bath spin interactions.

#### A. Trace distance

We observe the effect of interaction of bath spins over the dynamics of the central spin, both in single qubit and two qubit central spin models. Trace distance gives a measure of the distinguishability between two quantum states, and is given by

$$T(\rho_1, \rho_2) = \frac{1}{2} \text{Tr} \sqrt{(\rho_1 - \rho_2)^\dagger (\rho_1 - \rho_2)}. \quad (25)$$

We first calculate the trace distance between the single qubit central spin systems for the (non-)interacting bath spins. We take the initial state in both cases to be  $|1\rangle$  and plot the trace distance between  $\rho_S$  and  $\rho'_S$  from Eq. (5) and Eq. (16), respectively, in Fig. (1). The impact of bath spin interactions on

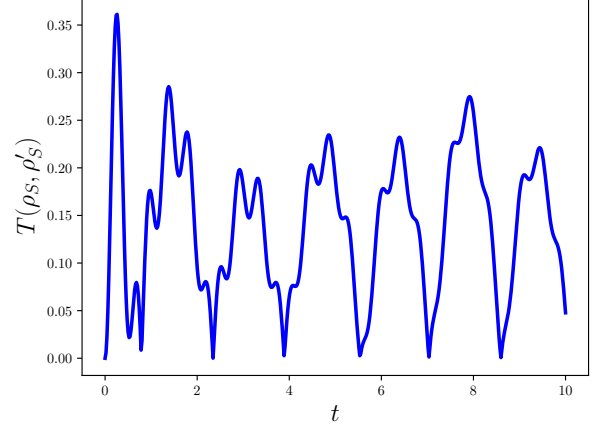


FIG. 1. Variation of trace distance ( $T(\rho_S, \rho'_S)$ ) between single qubit central spin states when interaction in bath spins is turned on or off. The parameters have following values:  $\epsilon = 1$ ,  $\omega = 2$ ,  $\omega_0 = 2$ ,  $N = 100$ ,  $T = 1$ .

the single qubit central spin system is clearly brought out and is seen to be non-monotonic.

For the two qubit central spin system, we consider the initial state to be  $|11\rangle$ . In the global bath scenario, we calculate the trace distance between the states  $\rho_{S_1 S_2}$  and  $\rho'_{S_1 S_2}$  given in Eq. (20) and Eq. (24), respectively. Fig. (2) depicts the difference in evolution between the cases, where the individual bath spins are interacting or not. In the local bath scenario, we calculate the trace distance between states  $\rho_{AB}$  and  $\rho'_{AB}$  from Eq. (17) and Eq. (18), respectively. Trace distance plotted in Fig. (3) again shows the difference in the evolution of the system caused by the interaction among the spins of the individual baths. A comparison between the above figures reveals that while the trace distance can be zero at certain times for the single central spin model, it is not so for the two qubit central spin model.

#### B. von Neumann entropy

For a given state  $\rho$  of a quantum system, the von Neumann entropy of the system is given as

$$S(\rho) = -\text{Tr}(\rho \log \rho). \quad (26)$$

In the single spin case, taking the initial state to be  $|1\rangle$ , the von Neumann entropy of the states is calculated using Eq. (5) and Eq. (16). Figure (4) depicts the difference in the evolution of von Neumann entropy for the single qubit central spin model for (a). where the bath spins interact and (b). where they do not interact with each other. For the non interacting bath

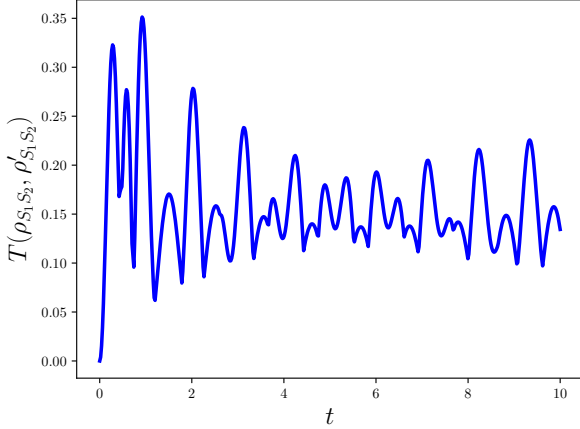


FIG. 2. Variation of trace distance ( $T(\rho_{S_1 S_2}, \rho'_{S_1 S_2})$ ) between two qubit central spin states, in global bath scenario, when interaction in bath spins is turned on or off. The parameters are:  $\epsilon_1 = 2.4$ ,  $\epsilon_2 = 2.5$ ,  $\omega_1 = 3.0$ ,  $\omega_2 = 3.1$ ,  $\omega_a = 2.0$ ,  $\omega_b = 2.1$ ,  $\delta = 4$ ,  $M = 25$ ,  $N = 25$ ,  $T = 1$ .

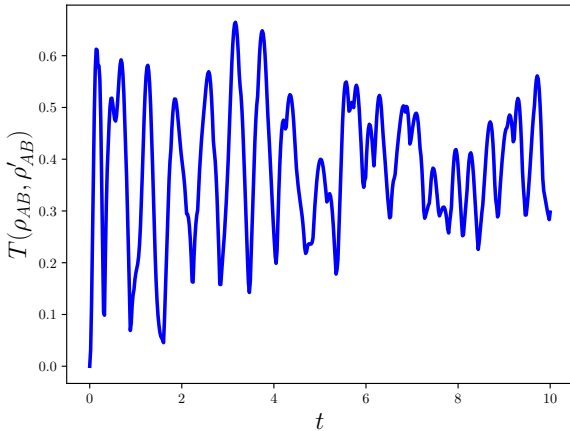


FIG. 3. Variation of trace distance ( $T(\rho_{AB}, \rho'_{AB})$ ) between two qubit central spin systems, in local bath scenario, when interaction in bath spins is turned on or off. The parameters have following values:  $\epsilon_1 = 2.4$ ,  $\epsilon_2 = 2.5$ ,  $\omega_1 = 3.0$ ,  $\omega_2 = 3.1$ ,  $\omega_a = 2.0$ ,  $\omega_b = 2.1$ ,  $M = 25$ ,  $N = 25$ ,  $T = 1$ .

spins scenario, the von Neumann entropy quickly reaches the maximum value, with small fluctuations, that is, the evolution of the state is close to a maximally mixed state. In contrast, for the interacting bath spins, we see larger variation in the von Neumann entropy depicting a larger exchange of information between the bath and the central spin.

In the two qubit case, we consider the initial state of the central spin system to be  $|11\rangle$  and calculate the von Neumann entropy for both local bath and global bath scenarios. Figure (5a), depicts the von Neumann entropy for the local bath scenario, while the Fig. (5b) illustrates the global bath scenario. For both cases, we see a greater variation of von Neumann

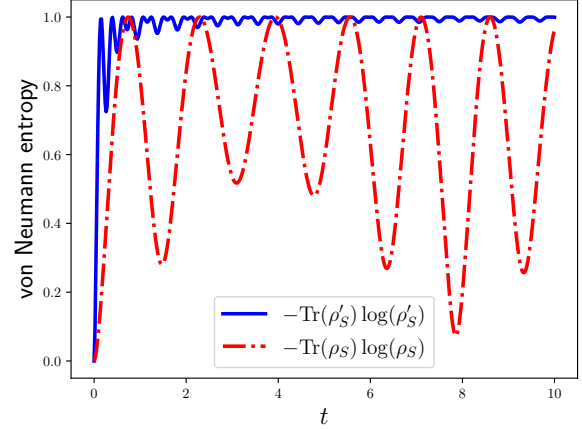


FIG. 4. Variation of von Neumann entropy with time in single qubit central spin model. Solid blue line corresponds to the case where bath spins do not interact among themselves and dot-dashed red line corresponds to the case where bath spins interact with each other. The parameters have following values:  $\epsilon = 1$ ,  $\omega = 2$ ,  $\omega_0 = 2$ ,  $N = 100$ ,  $T = 1$ .

entropy in the case of interacting bath spins. The variation in the von Neumann entropy approaches a fixed value when bath spins are non-interacting. One can also observe from the above figures that the von Neumann entropy for the single qubit and two qubit models (in local bath scenario), follow a similar pattern, where the evolution quickly takes the system to a maximally mixed state, modulo small fluctuations, when bath spins are non-interacting. However, the evolution of von Neumann entropy is different for the two qubit model in global bath scenario. Further, in the time window shown, the global dynamics does not evolve the initial state to the maximally mixed state, in contrast to the local dynamics. These highlight the difference between the local and global bath dynamics, in consistency with the observation in [51].

#### IV. QUANTUM SPEED LIMIT TIME

The bound for the minimum time required for a quantum system to evolve between two states is defined by quantum speed limit (QSL) time. Different quantum state distinguishability measures are available to estimate the quantum speed limit time for the non-unitary evolution between two arbitrary states [53, 54]. Mandelstamm-Tamm type bound [53] based on the relative purity of quantum states for the open quantum system is given by

$$\tau \geq \tau_{QSL} = \frac{2\theta^2}{\pi^2} \frac{\sqrt{\text{tr}\rho_0^2}}{\sum_{\alpha} \|K_{\alpha}(t, 0)\rho_0\dot{K}_{\alpha}^{\dagger}(t, 0)\|}, \quad (27)$$

where  $\theta = \cos^{-1}[\mathcal{P}(t)]$  with  $\theta \in [0, \pi/2]$ ,  $\mathcal{P}(t) = \text{tr}(\rho_t \rho_0) / \text{tr}(\rho_0^2)$  is the relative purity of initial and final states. We have  $\bar{X} = \tau^{-1} \int_0^{\tau} X dt$ , and  $\|A\| = \sqrt{\text{tr}(A^{\dagger}A)}$  is the Hilbert-Schmidt

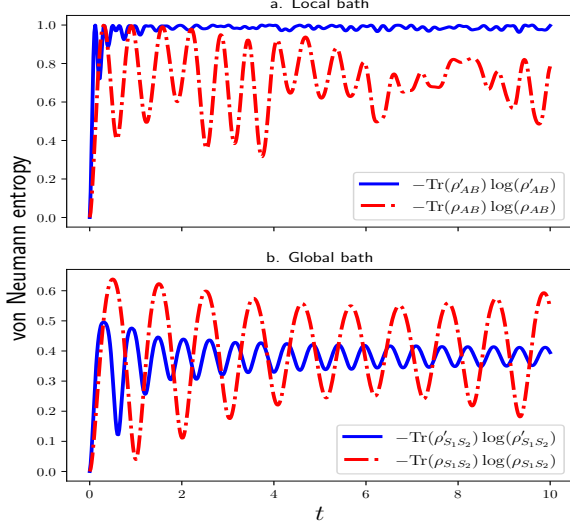


FIG. 5. Variation of von Neumann entropy with time in two qubit central spin model. Subplot (a) refers to the local bath scenario and (b) refers to the global bath scenario. Solid blue line corresponds to the case where bath spins do not interact among themselves and dot-dashed red line corresponds to the case where bath spins interact with each other. The parameters are:  $\epsilon_1 = 2.4$ ,  $\epsilon_2 = 2.5$ ,  $\omega_1 = 3.0$ ,  $\omega_2 = 3.1$ ,  $\omega_a = 2.0$ ,  $\omega_b = 2.1$ ,  $M = 25$ ,  $N = 25$ ,  $T = 1$ .

norm of  $A$ . Using Eq. (27), we estimate the speed limit time for the dynamics of interacting and non-interacting central spin systems, and their behavior are investigate for different sizes of bath spins. We also discuss the connection between quantum speed limit time and quantum correlations for local and global bath effects. To begin with, we consider the dynamics of  $\tau_{QSL}$  for the single qubit central spin model for an initial state  $|1\rangle$ . In Fig. (6), we see that as we increase the size of the bath, in the case of non-interacting bath spins, the QSL time decreases, or in other words, the evolution of the system between two states is faster. In the case of interacting bath spins, we observe very small change in the QSL time as we increase the number of bath spins.

The effect of the central spin-bath interaction parameter ( $\epsilon$ ) on QSL time for single qubit central spin system, can be seen in Fig. (7). In the case of non-interacting bath spins, the frequency of oscillation of  $\tau_{QSL}$  rapidly increases on increasing the number of bath spins. However, when the bath spins are interacting, the behaviour of QSL time is nearly same for different number of spins in the bath.

## V. QUANTUM CORRELATIONS

Entanglement is one of the most important resources in quantum information. Concurrence is an entanglement measure for a two qubit system [55], defined as

$$C(\rho_{AB}) = \max \{0, \lambda_1 - \lambda_2 - \lambda_3 - \lambda_4\}, \quad (28)$$

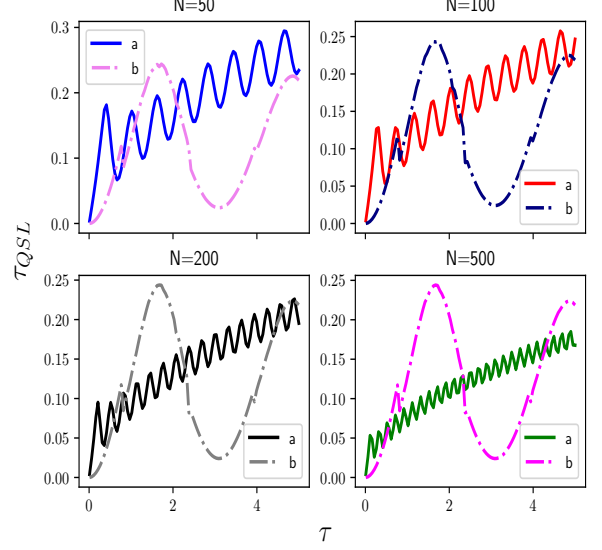


FIG. 6. Variation of the quantum speed limit time  $\tau_{QSL}$  with the driving time  $\tau$  for different number of bath spins. In each subplot, (a) corresponds to the case when bath spins do not interact with each other and (b) corresponds to the case when bath spins interact with each other. The parameters have following values:  $\epsilon = 1$ ,  $\omega = 2$ ,  $\omega_0 = 2$  and  $T = 1$ .

where  $\lambda_i$ 's are the eigenvalues of the matrix  $\sqrt{\sqrt{\rho_{AB}}\tilde{\rho}_{AB}\sqrt{\rho_{AB}}}$ , in decreasing order, and  $\tilde{\rho}_{AB} = (\sigma^x \otimes \sigma^y)\rho_{AB}^*(\sigma^x \otimes \sigma^y)$ . We calculate the concurrence for the evolution of the two central spins in the local bath scenario with interacting individual bath spins, as given in Eq. (17). If we consider the initial state of the system to be  $|\psi_{AB}\rangle = \frac{1}{\sqrt{2}}(|00\rangle + |11\rangle)$ , then at any time  $t$ , the state  $\rho_{AB}$  is given as

$$\rho_{AB}(t) = \begin{pmatrix} \rho_{11} & 0 & 0 & \rho_{14} \\ 0 & \rho_{22} & \rho_{23} & 0 \\ 0 & \rho_{23}^* & \rho_{33} & 0 \\ \rho_{14}^* & 0 & 0 & \rho_{44} \end{pmatrix}, \quad (29)$$

where the elements of the density matrix are given as

$$\rho_{11} = \frac{1}{2} \left[ d_{1A}(t)^2 d_{1B}(t)^2 + \left( \frac{T_{1A}^2 R_{1A}}{1 + T_{1A}^2} + \frac{T_{2A}^2 R_{2A}}{1 + T_{2A}^2} \right) \times \left( \frac{T_{1B}^2 R_{1B}}{1 + T_{1B}^2} + \frac{T_{2B}^2 R_{2B}}{1 + T_{2B}^2} \right) \right], \quad (30)$$

$$\rho_{22} = \frac{1}{2} \left[ b_{1B}(t)^2 \left( \frac{T_{1A}^2 R_{1A}}{1 + T_{1A}^2} + \frac{T_{2A}^2 R_{2A}}{1 + T_{2A}^2} \right) + d_{1A}(t)^2 \times \left( \frac{R_{1B}}{1 + T_{1B}^2} + \frac{R_{2B}}{1 + T_{2B}^2} \right) \right], \quad (31)$$

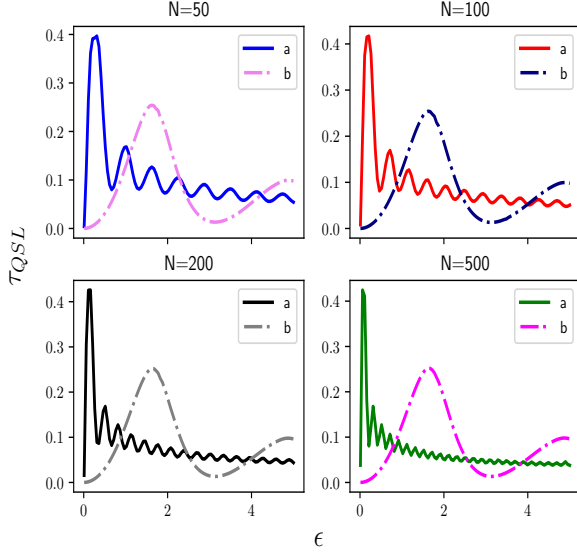


FIG. 7. Quantum speed limit time  $\tau_{QSL}$  with the central spin and bath interaction parameter,  $\epsilon$  for different number of bath spins. In each subplot, (a) corresponds to the case when bath spins do not interact with each other and (b) corresponds to the case when bath spins interact with each other. The parameters are chosen to be:  $\omega = 2$ ,  $\omega_0 = 2$ ,  $\tau = 1$  and  $T = 1$ .

$$\rho_{33} = \frac{1}{2} \left[ b_{1A}(t)^2 \left( \frac{T_{1B}^2 R_{1B}}{1 + T_{1B}^2} + \frac{T_{2B}^2 R_{2B}}{1 + T_{2B}^2} \right) + d_{1B}(t)^2 \times \left( \frac{R_{1A}}{1 + T_{1A}^2} + \frac{R_{2A}}{1 + T_{2A}^2} \right) \right], \quad (32)$$

$$\rho_{44} = \frac{1}{2} \left[ b_{1A}(t)^2 b_{1B}(t)^2 + \left( \frac{R_{1A}}{1 + T_{1A}^2} + \frac{R_{2A}}{1 + T_{2A}^2} \right) \times \left( \frac{R_{1B}}{1 + T_{1B}^2} + \frac{R_{2B}}{1 + T_{2B}^2} \right) \right], \quad (33)$$

$$\rho_{14} = \frac{1}{2} \left( \frac{R_{1A} T_{1A} e^{i\theta_A(t)}}{1 + T_{1A}^2} + \frac{R_{2A} T_{2A} e^{i\theta_A(t)}}{1 + T_{2A}^2} \right) \times \left( \frac{R_{1B} T_{1B} e^{i\theta_B(t)}}{1 + T_{1B}^2} + \frac{R_{2B} T_{2B} e^{i\theta_B(t)}}{1 + T_{2B}^2} \right), \quad (34)$$

and  $\rho_{23} = 0$ . The values of  $b_1(t)$ ,  $d_1(t)$ ,  $R_{1,2}(t)$  and  $T_{1,2}(t)$  are given in Eq. (7), Eq. (11) and Eq. (13), respectively. Subscripts  $A$  and  $B$  correspond to central spin  $A$  and central spin  $B$ , respectively. The density matrix in Eq. (29) has the form of a two qubit X state [56]. We can now write the concurrence for this state as

$$C(\rho_{AB}) = 2 \max\{0, |\rho_{23}| - \sqrt{\rho_{44}\rho_{11}}, |\rho_{14}| - \sqrt{\rho_{33}\rho_{22}}\}. \quad (35)$$

Using the same approach we can estimate the concurrence for the two central spins in the local bath with non-interacting individual bath spins.

Another well known measure of quantum correlation in a quantum system is quantum discord [57–60]. Here quantum

discord between the two central spins in the local bath scenario with interacting individual bath spins, defined in Eq. (17) is given by

$$\mathcal{D}(\rho_{AB}) = \mathcal{S}(\rho_B) - \mathcal{S}(\rho_{AB}) + \mathcal{S}(\rho_{A|B}), \quad (36)$$

where  $\mathcal{S}(\rho_B)$  is the von Neumann entropy of the subsystem of central spin  $B$ ,  $\mathcal{S}(\rho_{AB})$  is the joint von-Neumann entropy of the system  $\rho_{AB}$  and  $\mathcal{S}(\rho_{A|B})$  is the quantum conditional entropy of the system. Further, the quantum conditional entropy is given by

$$\mathcal{S}(\rho_{A|B}) = \min_{\{M_j\}} \sum_{j=1}^2 p_j \mathcal{S}(\rho_{A|M_j}), \quad (37)$$

where  $\rho_{A|M_j}$  is the reduced state of the subsystem  $A$  after a measurement is performed over subsystem  $B$  and  $M_j$ 's are the generalized measurement operators for subsystem  $B$ . For single qubit, these measurement operators are given by

$$M_1 = |u_B\rangle\langle u_B|, \quad M_2 = |v_B\rangle\langle v_B|, \quad (38)$$

where  $|u_B\rangle = \cos(\theta)|0\rangle + e^{i\phi}\sin(\theta)|1\rangle$ , and  $|v_B\rangle = \sin(\theta)|0\rangle - e^{i\phi}\cos(\theta)|1\rangle$  such that  $0 \leq \theta \leq \pi/2$  and  $0 \leq \phi \leq 2\pi$ . For a given state of the system  $\rho_{AB}$  in Eq. (29), quantum discord is given by

$$\begin{aligned} \mathcal{D}(\rho_{AB}) = & -(\rho_{11} + \rho_{33}) \log_2(\rho_{11} + \rho_{33}) - (\rho_{22} + \rho_{44}) \\ & \times \log_2(\rho_{22} + \rho_{44}) + \rho_{22} \log_2 \rho_{22} + \rho_{33} \log_2 \rho_{33} \\ & + \lambda_1 \log_2 \lambda_1 + \lambda_2 \log_2 \lambda_2 - \frac{\lambda_3}{2} \log_2 \left( \frac{\lambda_3}{2} \right) \\ & - \frac{\lambda_4}{2} \log_2 \left( \frac{\lambda_4}{2} \right), \end{aligned} \quad (39)$$

where

$$\begin{aligned} \lambda_1 &= \frac{(\rho_{11} + \rho_{44})}{2} + \frac{1}{2} \sqrt{(\rho_{11} - \rho_{44})^2 + 4|\rho_{14}|^2}, \\ \lambda_2 &= \frac{(\rho_{11} + \rho_{44})}{2} - \frac{1}{2} \sqrt{(\rho_{11} - \rho_{44})^2 + 4|\rho_{14}|^2}, \\ \lambda_3 &= 1 + \sqrt{(\rho_{11} - \rho_{33} + \rho_{22} - \rho_{44})^2 + 4|\rho_{14}|^2}, \\ \lambda_4 &= 1 - \sqrt{(\rho_{11} - \rho_{33} + \rho_{22} - \rho_{44})^2 + 4|\rho_{14}|^2}. \end{aligned} \quad (40)$$

The intermediate steps in the calculation of quantum discord are given in Appendix A. The quantum discord for the two central spin interacting with local baths, with non-interacting individual bath spins, can be obtained similarly.

## VI. CONNECTION BETWEEN QSL TIME AND QUANTUM CORRELATIONS

We first consider the dynamics of the two qubit central spin system in local bath scenario. Considering the initial state of the two central spins to be  $|\psi\rangle_{AB} = \frac{1}{2}(|00\rangle + |11\rangle)$ , we use Eq. (27) and dynamics of the state defined in Eq. (17) to calculate the QSL time of the system, in the case of the individual baths

of interacting spins and Eq. (18) to calculate the QSL time in case of individual baths of non-interacting spins. Further, we analyze the dynamics of the quantum correlations, in particular entanglement and quantum discord, in both of the aforementioned cases, as given in Sec. V. In Fig. (8), we see the

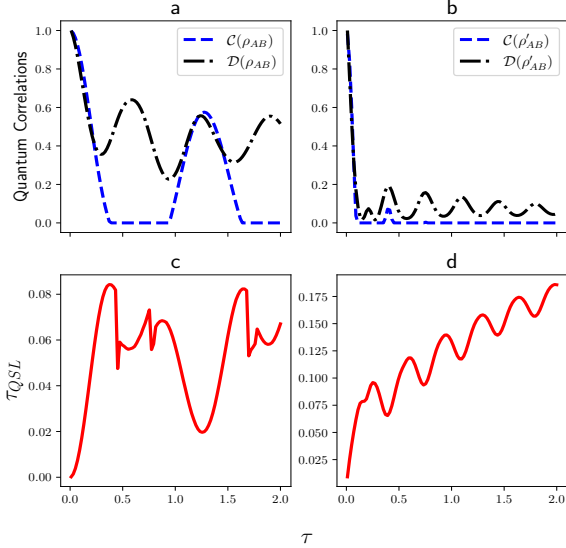


FIG. 8. Variation of the QSL time ( $\tau_{QSL}$ ) and quantum correlations, in local bath scenario, for the two qubit central spin model with time. In (a) and (c), the spins of the individual baths interact with each other while in (b) and (d), they do not interact with each other. The parameters are:  $\epsilon_1 = 2.4$ ,  $\epsilon_2 = 2.5$ ,  $\omega_1 = 3.0$ ,  $\omega_2 = 3.1$ ,  $\omega_a = 2.0$ ,  $\omega_b = 2.1$ ,  $M = 25$ ,  $N = 25$ ,  $T = 1$ .

changes in QSL time and quantum correlations *w.r.t.* time for the two qubit central spin model, in local bath scenario. We observe that the changes in dynamics of the quantum correlations are in contrast with the changes in QSL time, for both the cases of interacting and non-interacting individual bath spins. This suggests that the speed of the evolution of the system is aided by increments in the quantum correlations, in that the blips in quantum correlations corresponds to the dips in QSL time.

We next consider the case of two qubit central spin model in the global bath scenario, defined by the Hamiltonians given in Eq. (19) and Eq. (21). Considering the initial state of the coupled central spins as  $|\psi\rangle_{S_1 S_2} = \frac{1}{\sqrt{2}}(|00\rangle + |11\rangle)$ , we first analyze the dynamics of QSL time and quantum correlations for a given central spin-spin interaction strength ( $\delta$ ), with time. In Fig. (9), we witness that the changes in the dynamics of quantum correlations are again in contrast with the changes in QSL time for both the cases of interacting and non-interacting individual bath spins. Once again it is observed that the increment in quantum correlations facilitates the speed of the evolution of the system. We next see the impact of the interaction strength between the two central spins on the QSL time and quantum correlations at a given time. In Fig. (10), we observe that the quantum correlations in the system increases as the interaction strength between the two central spins in-

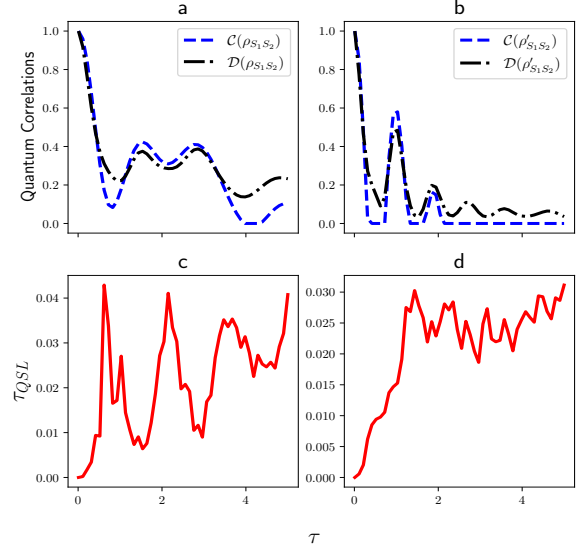


FIG. 9. QSL time ( $\tau_{QSL}$ ) and quantum correlations, in global bath scenario, for the two qubit central spin model with time. In (a) and (c), the spins of the individual baths interact with each other while in (b) and (d), they do not interact with each other. The parameters are chosen to be:  $\omega_1 = 2.0$ ,  $\omega_2 = 1.9$ ,  $\omega_a = 1.1$ ,  $\omega_b = 1.2$ ,  $\delta = 2$ ,  $\epsilon_1 = 2.0$ ,  $\epsilon_2 = 2.0$ ,  $M = 15$ ,  $N = 15$  and  $T = 1$ .

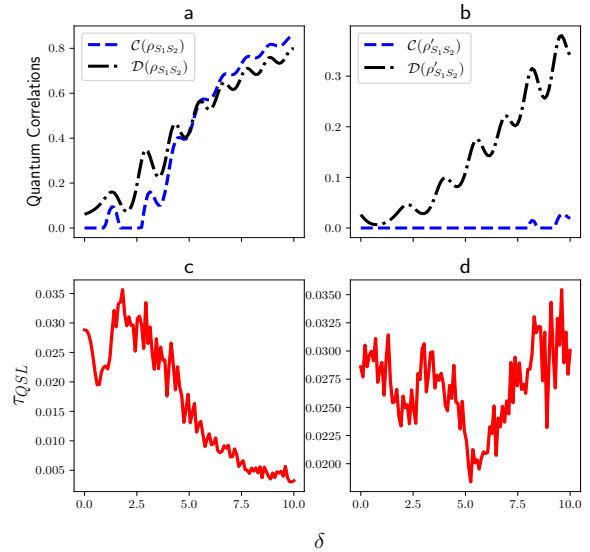


FIG. 10. Variation of the QSL time ( $\tau_{QSL}$ ) and quantum correlations, in global bath scenario, for the two qubit central spin model with the interaction strength between central spins  $\delta$ . In (a) and (c), the spins of the individual baths interact with each other while in (b) and (d), they do not interact with each other. The parameters have following values:  $\omega_1 = 2.0$ ,  $\omega_2 = 1.9$ ,  $\omega_a = 1.1$ ,  $\omega_b = 1.2$ ,  $\tau = 6$ ,  $\epsilon_1 = 2.0$ ,  $\epsilon_2 = 2.0$ ,  $M = 15$ ,  $N = 15$  and  $T = 1$ .

creases, which is true for both the cases of interacting and non-interacting spins of the individual baths. Here again the



speed of the evolution of the system is faster when quantum correlations increase. It can also be observed that higher interaction strength between the two central spins, for the non-interacting individual bath spins case, revives entanglement and QSL time even at higher driving times, as can be seen from Figs. (10b, 10d). A general remark that can be made from the above figures is that there are regimes in the parameter space where the entanglement is zero but quantum discord is non-zero. In fact we can see that in general, interaction in the bath spins aid in the generation of quantum correlations.

## VII. CONCLUSIONS

Here we have focused on the different types of single qubit and two qubit central spin models. Special emphasis is laid on whether the bath spins interact or are non-interacting. For the two qubit central spin model, we have considered the cases whether or not the central spins interact with each other. These are called the global or local bath scenarios, respectively. The operator-sum representations are provided for all the models. Trace distance and von Neumann entropy have been used to characterize these models. We have observed that the interaction of bath spins plays an important role in the dynamics of the system. The evolution of the single and two qubit (in the local bath scenario) central spin models, where bath spins are non-interacting, are seen to evolve into a nearly maximally mixed state. The impact of bath size on the QSL time for the single qubit model brought out that in the case of non-interacting bath spins, the QSL time is impacted, but the effect was not prominent for the case of interacting bath spins. Further, we have studied the dynamics of quantum correlations, particularly entanglement and quantum discord, in the two qubit central spin models. A connection was observed between the QSL time and quantum correlations revealing that the higher quantum correlations can result in faster speed of evolution of the system.

## ACKNOWLEDGEMENTS

SB acknowledges support from Interdisciplinary Cyber Physical Systems (ICPS) programme of the

Department of Science and Technology (DST), India, Grant No.: DST/ICPS/QuST/Theme-1/2019/6 and DST/ICPS/QuST/Theme-1/2019/13. SB also acknowledges support from the Interdisciplinary Research Platform (IDRP) on Quantum Information and Computation (QIC) at IIT Jodhpur.

## Appendix A: Intermediate steps in the calculation of quantum discord

The reduced subsystem for central spin  $B$ , from Eq. (17), is given by

$$\rho_B = \text{Tr}_A(\rho_{AB}) = \begin{pmatrix} \rho_{11} + \rho_{33} & 0 \\ 0 & \rho_{22} + \rho_{44} \end{pmatrix}. \quad (\text{A1})$$

From the eigenvalues of the density matrix above, the von Neumann entropy of the reduced subsystem for central spin  $B$  is written as

$$\mathcal{S}(\rho_B) = -(\rho_{11} + \rho_{33}) \log_2(\rho_{11} + \rho_{33}) - (\rho_{22} + \rho_{44}) \log_2(\rho_{22} + \rho_{44}), \quad (\text{A2})$$

Further, from the eigenvalues of the density matrix given in Eq. (17), the joint entropy of the two qubit central spin system in local bath is given as

$$\mathcal{S}(\rho_{AB}) = -\rho_{22} \log_2 \rho_{22} - \rho_{33} \log_2 \rho_{33} - \lambda_1 \log_2 \lambda_1 - \lambda_2 \log_2 \lambda_2, \quad (\text{A3})$$

where  $\lambda_1$  and  $\lambda_2$  as given in Eq. (40). In the next step, we optimize Eq. (37) based upon the measurement operators given in Eq. (38), to write the quantum conditional entropy of the system in Eq. (17) as

$$\mathcal{S}(\rho_{A|B}) = -\frac{\lambda_3}{2} \log_2 \left( \frac{\lambda_3}{2} \right) - \frac{\lambda_4}{2} \log_2 \left( \frac{\lambda_4}{2} \right), \quad (\text{A4})$$

where  $\lambda_3$  and  $\lambda_4$  are as in Eq. (40).

- 
- [1] H. P. Breuer and F. Petruccione, *The theory of open quantum systems* (Oxford University Press, Great Clarendon Street, 2002).
  - [2] S. Banerjee, *Open Quantum Systems* (Springer Singapore, 152 Beach Rd, 21-01 Gateway East, Singapore 189721, 2018).
  - [3] W. H. Louisell, *Quantum Statistical Properties of Radiation* (1990).
  - [4] G. S. Agarwal, *Quantum Optics* (Cambridge University Press, 2012).
  - [5] U. Weiss, *Quantum Dissipative Systems*, 2nd ed., Series in Modern Condensed Matter Physics, Vol. 10 (World Scientific, 1999).
  - [6] A. Caldeira and A. Leggett, *Annals of Physics* **149**, 374 (1983).
  - [7] H. Grabert, P. Schramm, and G.-L. Ingold, *Physics Reports* **168**, 115 (1988).
  - [8] S. Banerjee and R. Ghosh, *Phys. Rev. A* **62**, 042105 (2000).
  - [9] S. Banerjee and R. Ghosh, *Phys. Rev. E* **67**, 056120 (2003).
  - [10] S. Umasankar, A. K. Alok, and S. Banerjee, *PoS EPS-HEP2015*, 578 (2016).
  - [11] S. Banerjee, A. K. Alok, and R. MacKenzie, *The European Physical Journal Plus* **131**, 1 (2016).
  - [12] J. Naikoo, A. K. Alok, and S. Banerjee, *Phys. Rev. D* **97**, 053008 (2018).

- [13] K. Dixit, J. Naikoo, S. Banerjee, and A. K. Alok, *The European Physical Journal C* **79**, 1 (2019).
- [14] S. Banerjee, A. Kumar Alok, S. Omkar, and R. Srikanth, *Journal of High Energy Physics* **2017**, 1 (2017).
- [15] S. Omkar, S. Banerjee, R. Srikanth, and A. K. Alok, *Quantum Information and Computation* **16**, 757 (2016).
- [16] B. L. Hu and A. Matacz, *Phys. Rev. D* **49**, 6612 (1994).
- [17] C. Singha and S. Banerjee, *Phys. Rev. D* **105**, 045020 (2022).
- [18] Y. Tanimura, *The Journal of Chemical Physics* **153**, 020901 (2020), <https://doi.org/10.1063/5.0011599>.
- [19] K. H. Hughes, C. D. Christ, and I. Burghardt, *The Journal of Chemical Physics* **131**, 124108 (2009), <https://doi.org/10.1063/1.3226343>.
- [20] J. Iles-Smith, N. Lambert, and A. Nazir, *Phys. Rev. A* **90**, 032114 (2014).
- [21] S. Huelga and M. Plenio, *Contemporary Physics* **54**, 181 (2013), <https://doi.org/10.1080/00405000.2013.829687>.
- [22] I. Chakrabarty, S. Banerjee, and N. Siddharth, *Quantum Inf. Comput.* **11**, 541 (2011).
- [23] U. Shrikant, R. Srikanth, and S. Banerjee, *Phys. Rev. A* **98**, 032328 (2018).
- [24] S. Utagi, R. Srikanth, and S. Banerjee, *Quantum Information Processing* **19**, 1 (2020).
- [25] G. Thomas, N. Siddharth, S. Banerjee, and S. Ghosh, *Phys. Rev. E* **97**, 062108 (2018).
- [26] S. Banerjee, C. M. Chandrashekar, and A. K. Pati, *Phys. Rev. A* **87**, 042119 (2013).
- [27] S. Banerjee and R. Srikanth, *The European Physical Journal D* **46**, 335 (2008).
- [28] C. Chandrashekar and S. Banerjee, *Physics Letters A* **375**, 1553 (2011).
- [29] S. Bhattacharya, S. Banerjee, and A. K. Pati, *Quantum Information Processing* **17**, 1 (2018).
- [30] B. Vacchini, A. Smirne, E.-M. Laine, J. Piilo, and H.-P. Breuer, *New Journal of Physics* **13**, 093004 (2011).
- [31] H.-P. Breuer, E.-M. Laine, J. Piilo, and B. Vacchini, *Rev. Mod. Phys.* **88**, 021002 (2016).
- [32] Á. Rivas, S. F. Huelga, and M. B. Plenio, *Reports on Progress in Physics* **77**, 094001 (2014).
- [33] M. J. W. Hall, J. D. Cresser, L. Li, and E. Andersson, *Phys. Rev. A* **89**, 042120 (2014).
- [34] S. Utagi, R. Srikanth, and S. Banerjee, *Scientific Reports* **10**, 1 (2020).
- [35] A. Shabani and D. A. Lidar, *Phys. Rev. A* **71**, 020101 (2005).
- [36] J. Naikoo, S. Dutta, and S. Banerjee, *Phys. Rev. A* **99**, 042128 (2019).
- [37] J. Naikoo and S. Banerjee, *Quantum Information Processing* **19**, 1 (2020).
- [38] J. Naikoo, S. Banerjee, and R. Srikanth, *Quantum Information Processing* **19**, 1 (2020).
- [39] N. P. Kumar, S. Banerjee, R. Srikanth, V. Jagadish, and F. Petruccione, *Open Systems & Information Dynamics* **25**, 1850014 (2018), <https://doi.org/10.1142/S1230161218500142>.
- [40] K. G. Paulson, E. Panwar, S. Banerjee, and R. Srikanth, *Quantum Information Processing* **20**, 1 (2021).
- [41] S. Deffner and S. Campbell, *Journal of Physics A: Mathematical and Theoretical* **50**, 453001 (2017).
- [42] K. G. Paulson, S. Banerjee, and R. Srikanth, *arXiv preprint arXiv:2107.03306* (2021).
- [43] K. G. Paulson and S. Banerjee, *arXiv preprint arXiv:2202.08078* (2022).
- [44] N. V. Prokofev and P. C. E. Stamp, *Reports on Progress in Physics* **63**, 669 (2000).
- [45] J. Parkinson and D. Farnell, *An Introduction to Quantum Spin Systems: Preface*, Lecture Notes in Physics, Vol. 816 (Springer Nature, United States, 2010).
- [46] T. F. Rosenbaum, *Journal of Physics: Condensed Matter* **8**, 9759 (1996).
- [47] A. J. Leggett, S. Chakravarty, A. T. Dorsey, M. P. A. Fisher, A. Garg, and W. Zwerger, *Rev. Mod. Phys.* **59**, 1 (1987).
- [48] J. Ordonez-Miranda, Y. Ezzahri, and K. Joulain, *Phys. Rev. E* **95**, 022128 (2017).
- [49] C. Mukhopadhyay, S. Bhattacharya, A. Misra, and A. K. Pati, *Phys. Rev. A* **96**, 052125 (2017).
- [50] S. Bhattacharya and S. Banerjee, *Quanta* **10**, 55 (2021).
- [51] D. Tiwari, S. Datta, S. Bhattacharya, and S. Banerjee, *arXiv preprint arXiv:2205.04135* (2022).
- [52] G. Değordi and A. Vidiella-Barranco, *Optics Communications* **387**, 366 (2017).
- [53] A. del Campo, I. L. Egusquiza, M. B. Plenio, and S. F. Huelga, *Phys. Rev. Lett.* **110**, 050403 (2013).
- [54] M. M. Taddei, B. M. Escher, L. Davidovich, and R. L. de Matos Filho, *Phys. Rev. Lett.* **110**, 050402 (2013).
- [55] W. K. Wootters, *Phys. Rev. Lett.* **80**, 2245 (1998).
- [56] S. R. Hedemann, *Quantum Information Processing* **17**, 1 (2018).
- [57] H. Ollivier and W. H. Zurek, *Phys. Rev. Lett.* **88**, 017901 (2001).
- [58] M. Ramkarthik, D. Tiwari, and P. Barkataki, *International Journal of Theoretical Physics* **59**, 4040 (2020).
- [59] S. Adhikari and S. Banerjee, *Phys. Rev. A* **86**, 062313 (2012).
- [60] L. Henderson and V. Vedral, *Journal of Physics A: Mathematical and General* **34**, 6899 (2001).